small methods
www.small-methods.com

Micromechanical Indentation Platform for Rapid Analysis of Viscoelastic Biomolecular Hydrogels

*Phillip Lemke, Svenja Moench, Paula S. Jäger, Claude Oelschlaeger, Kersten S. Rabe, Carmen M. Domínguez, and Christof M. Niemeyer**

The advent of biomedical applications of soft bioinspired materials has entailed an increasing demand for streamlined and expedient characterization methods meant for both research and quality control objectives. Here, a novel measurement system for the characterization of biological hydrogels with volumes as low as 75 µL was developed. The system is based on an indentation platform equipped with micrometer drive actuators that allow the determination of both the fracture points and Young's moduli of relatively stiff polymers, including agarose, as well as the measurements of viscosity for exceptionally soft and viscous hydrogels, such as DNA hydrogels. The sensitivity of the method allows differentiation between DNA hydrogels produced by rolling circle amplification based on different template sequences and synthesis protocols. In addition, the polymerization kinetics of the hydrogels can be determined by time-resolved measurements, and the apparent viscosities of even more complex DNA-based nanocomposites can be measured. The platform presented here thus offers the possibility to characterize a broad variety of soft biomaterials in a targeted, fast, and cost-effective manner, holding promises for applications in fundamental materials science and ensuring reproducibility in the handling of complex materials.

1. Introduction

Biocompatible hydrogels are often made from synthetic or biomolecular polymers. They contain a porous 3D structure with high water content and tissue-like elastic properties that allow effective permeation of oxygen and nutrients, which is critical for cell colonization and tissue engineering applications.[1] While synthetic hydrogels may suffer from potential drawbacks due to adverse effects of chemical ingredients,[2] hydrogel materials from biomolecules, such as saccharides, peptides, proteins, or even nucleic acids, offer advantages in this respect, as they can be produced using exclusively non-toxic biochemical reactions. Biomolecular hydrogels of DNA have recently attracted considerable interest, as these biopolymers can also be programmed very efficiently via their nucleic acid sequence to install shape memory persistence, molecular recognition capabilities, and stimulus sensitivity, for example, to facilitate their biodegradation by enzymes. This is highly relevant to a variety of biomedical applications, particularly in the area of drug delivery.[3]

Since DNA hydrogels are functional polymer scaffolds that respond to stimuli, they can be structurally reconfigured using various physical or chemical triggers on the crosslinking units to control the stiffness of the hydrogels.[3e] In order to characterize the physical material properties, classical rheological methods such as steady-state shear rheology, dynamic rheology, and extensional rheology can be used,[3a-c,e] as well as sophisticated methods based, for example, on optical particle tracking techniques.[4] While classical methods have the disadvantage of requiring relatively large sample volumes of the expensive and very soft DNA material, the optical particle tracking-based methods are often limited to narrow local areas of the material, which can lead to inaccurate or incorrect results.[5] Both approaches make measurements of bulk properties over time, e.g., in the course of a polymerization reaction, very difficult to accomplish.

Instrumented indentation testing, also referred to as depth-sensitive indentation or nanoindentation, is progressively employed to characterize the mechanical properties of biological materials, polymers, ceramics, and metals. This method provides

P. Lemke, S. Moench, P. S. Jäger, K. S. Rabe, C. M. Domínguez, C. M. Niemeyer
Karlsruhe Institute of Technology (KIT)
Institute for Biological Interfaces (IBG 1)
Hermann-von-Helmholtz-Platz 1, 76344 Eggenstein-Leopoldshafen, Germany
E-mail: niemeyer@kit.edu
C. Oelschlaeger
Karlsruhe Institute of Technology (KIT)
Institute for Mechanical Process Engineering and Mechanics
Gotthard-Franz-Straße 3, 76131 Karlsruhe, Germany

The ORCID identification number(s) for the author(s) of this article can be found under https://doi.org/10.1002/smtd.202400251

DOI: 10.1002/smtd.202400251

valuable insights into the fundamental mechanisms governing mechanical behavior at micrometer and even submicrometer length scales in both soft biomaterials and hard materials alike.[6] For example, the method is frequently performed using atomic force microscopy (AFM) at smaller length scales (μm, nm), through static or dynamic oscillatory indentations.[7] However, determining the contact point between the indenter and certain hydrogels, essential for subsequent data analysis, can pose significant challenges due to their exceptionally soft nature. Moreover, AFM setups have been utilized for assessing fluid viscosity through the measurement of the thermal fluctuations of cantilevers immersed in such fluids.[8] It is worth noting though that AFM methods are associated with considerable costs and require in-depth specialist knowledge and time both for carrying out the measurements and for interpreting the results. To circumvent the above-mentioned weaknesses of established methods for rheological evaluation of the properties of low-viscosity materials, such as DNA and protein hydrogels, and to enable rapid in situ investigation of such materials with high-throughput, we report here on a computer-controlled micromechanical platform consisting of a plunger mounted on a load cell and an indentation vessel. Using agarose hydrogels and water-glycerol mixtures for calibration, we show that our device can reliably determine the elastic modulus and viscosity of various materials, and we apply it to characterize low-viscosity DNA hydrogels formed during biochemical polymerization.

2. Results and Discussion

2.1. Design of the Indentation Platform

The technical platform we have developed for indentation measurements of various materials, including hydrogels and viscous liquids, is illustrated in **Figure 1** with a photographic image (A) and 3D technical models (B). The platform consists of a plunger (I) against which a sample is moved during measurement, causing it to indent gel-like materials or displace viscous liquids, respectively, so that both compressive stress and viscosity measurements can be carried out. The plunger is attached to a standard load cell (II), which has been selected according to the sensitivity required for the application. If necessary, the load cell can be easily replaced to adapt the measuring platform to the force range required for specific sample materials. The load cell is connected to a Wheatstone bridge (III), which measures the small ohmic resistance changes induced by the load cell strain and transmits the signal to a computer. Before measurements were carried out, the load cell was calibrated with defined weights in order to convert the electrical signal into the corresponding force for the subsequent measurements (Figure S1, Supporting Information).

The sample-holding indentation vessels (IV) were inserted into an adapter plate (V). In order to achieve maximum variability and adaptability to the material to be analyzed, also with regard to the required volume, both different adapter plates and sample vessels of different sizes can be used. In particular, the combination of sample vessel and a plunger size suitable for the measurement allows, for example, samples with a volume of <75 μL to be used for viscosity measurements, which is not possible with conventional rheological methods that require milliliter-sized samples. This highly variable design underlines the flexibility of the platform presented here.

For the measurements performed in this work, plungers with a diameter of 1 and 4.3 mm were used, which were produced by micromilling from polymethylmethacrylate (PMMA) (Figure 1C,Ia,Ib). The 1 mm plunger was used for indentation measurements of rather stiff materials, such as agarose gels, which were filled into larger sample vessels with a diameter of 25 mm (Figure 1C,IVa) in order to minimize edge effects on the compressibility of the test material during the measurements. For viscosity measurements, on the other hand, the 4.3 mm plunger was used in combination with a sample vessel with a diameter of 4.5 mm (Figure 1C,IVb), whereby the liquid or viscous material under investigation is displaced through the resulting small gap, so that additional edge effects such as friction and capillary forces contribute to the measured indentation force. Additional technical details on the plunger and sample wells can be found in the Supporting Information, Figures S2 and S3 (Supporting Information).

The adapter plate was embedded in a precisely fitting base plate (VI) to enable a temperature setting with a resolution limit of 0.1 °C and an accuracy of 0.2 °C after calibration with a laboratory thermometer in accordance with DIN 12775 using a heating foil (VII) in combination with a thermostat module (VIII). Since viscosity measurements are highly temperature-dependent and precise temperature control is essential for the reproducibility of the measurements, the temperature sensor (IX) was inserted in the middle of the adapter plate so that the temperature is displayed at the level of the samples to be measured. The adapter plate (V) and the base plate (VI) were 3D-printed from the plastic acrylonitrile-styrene-acrylate (ASA), while the sample vessels (IV) were produced from PMMA by micromilling. Due to the materials used, these components have a low thermal conductivity (ASA: 0.17 W K^{-1} m^{-1}; PMMA: 0.19 W K^{-1} m^{-1}) and should be stable against any deformation in the temperature range considered here (4–37 °C, heat resistance up to 97 and 95 °C for ASA and PMMA, respectively). This resistance to temperature-induced deformation had to be ensured, as any deformation of the sample container during viscosity measurements would influence the result, since the small gap of 100 μm between the plunger and the vessel wall is crucial for the measurement signal.

Prior to all individual measurements, the platform and samples were brought to the target temperature, making low thermal conductivity of the system components and materials under investigation a non-critical factor. When the measurement temperature was reached, the measured values of the temperature module were stable over time due to the constant voltage applied to the heating foil before and during the measurements. Validation of the temperature inside the sample with an independent temperature measuring device showed the expected constant measurement temperature of 25 °C. At higher measuring temperatures (37 °C), however, the sample cooled down slowly. For future optimization of the system, it could therefore be advantageous to manufacture the platform parts from materials with improved thermal conductivity, such as aluminum (237 W K^{-1} m^{-1}), and/or to integrate the sample cell into a separate temperature-controlled compartment.

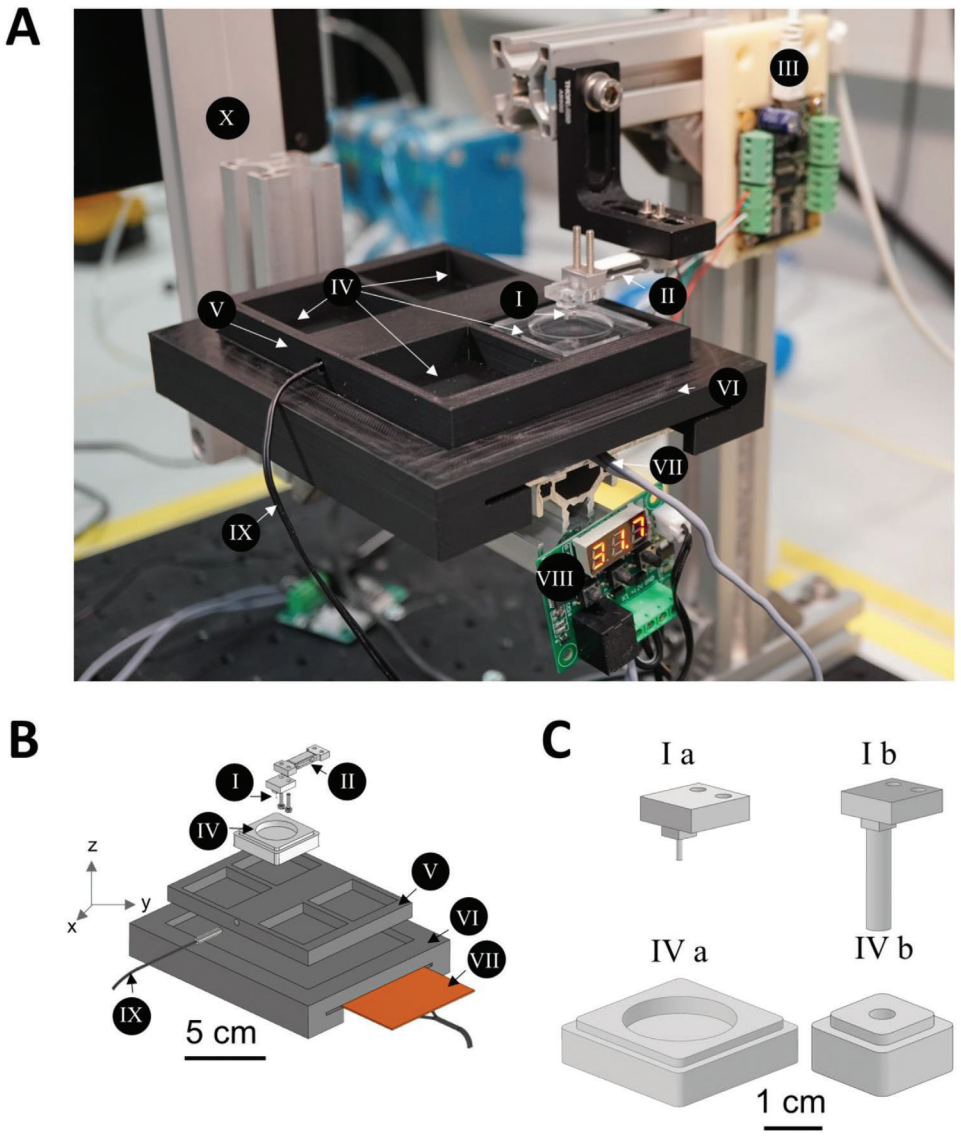

Figure 1. Platform for automated indentation measurements. A) Photographic and B) schematic illustration of the indentation platform. The Roman numerals indicate the plunger (I) for indentation, the load cell (II) for sensing the forces acting on the plunger, and the Wheatstone bridge (III) that converts the forces into electrical signals. Also marked are the components designed for flexible handling, including the sample vessel (IV), the adapter plate (V), the base plate (VI), was well as the heating foil (VII), thermostat module (VIII), and temperature sensor (IX) integrated for temperature control. All parts of the sample holder are attached to the freely positionable robotic arm (X) in order to bring the sample into contact with the load cell with spatial and temporal resolution. C) Schematic illustrations of the plungers and sample vessels used in this work. For detailed technical drawings see Figures S2 and S3 (Supporting Information).

The entire configuration was mounted on a positioning system that we had previously developed for lateral high-resolution sampling from microfluidic reactors[9] and which includes a robotic arm (X) that can move in three dimensions (x, y, z) with micrometer accuracy, a positioning error of <10 µm, and a bidirectional repeatability error of <2 µm. By securing the load cell in a fixed position while the platform with the sample vessels is in motion, vibrations caused by the movement of the positioning system are effectively isolated from the load cell. In addition, the robot can measure the exact distances traveled during indentation, which can be used to determine the penetration depth of the sample. Customized software was developed for this purpose, with which both the exact x-, y-, z-coordinates of the sample points and the desired sampling time can be defined, for example, to automatically measure the gelation of hydrogels in a time and spatially resolved manner. Overall, the platform presented here is a cost-effective setup in which all components can be purchased or easily manufactured. Further technical details about the assembly of the platform, temperature control, and a list of the components (Table S1, Supporting Information) can be found in the method section in the Supporting Information.

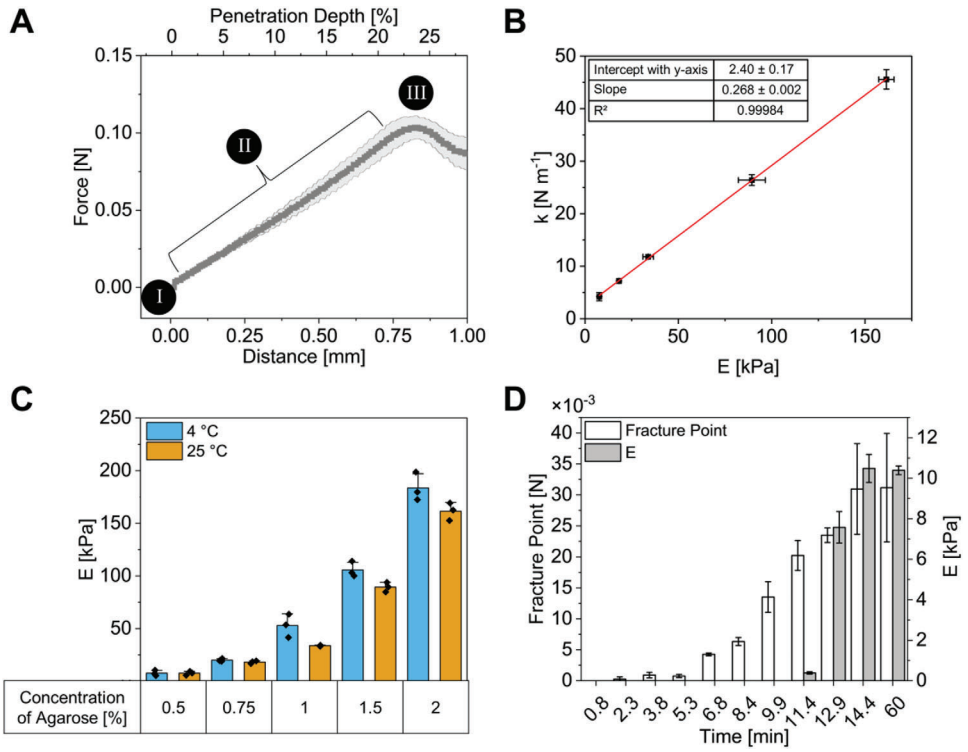

Figure 2. Indentation measurements of agarose gels. A) Representative force-distance curve measured with the here developed indentation platform. Contact point (I), continuous indentation phase (II), and fracture point (III) are depicted. For photographic illustration of these points, see Figure S4A (Supporting Information). B) Calibration of the indentation platform data using agarose gels with different concentrations (0.5–2 %) with a conventional rheometer. Note the very good fit of the model with a coefficient of determination R^2>0.99. C) Young's moduli (E) of agarose gels with different concentrations of agarose (0.5–2 %) gelled at either 4 °C (blue bars) or 25 °C (orange bars) determined with our indentation platform and measured in experimental triplicates. D) Time-resolved in situ measurement of gelation of a 0.5% agarose gel at a starting temperature of 37 °C with slow cooling to 27 °C within 15 min. Note that in the early phase of gelation, due to the low viscosity of the still liquid agarose solution, the fracture point (white bars) was used to evaluate the measurement results, while after about 12 min the gelation phase was almost complete and meaningful Young's moduli (grey bars) could be determined. All measurements (A–D) were conducted as experimental triplicates ($n = 3$) and plotted as mean ± standard deviation. The dots in inset (C) represent the individual measurements. For inset (D), the individual measurements can be found in Figure S6 (Supporting Information). Statistical analysis with the corresponding *p*-values can be found in Tables S3–S6 (Supporting Information).

2.2. Indentation Measurements of Agarose Gels

To evaluate the utility of our indentation platform for the characterization of gel-like materials, we first selected agarose gels that can be adjusted to a wide range of stiffnesses.[10] Agarose is a linear polysaccharide containing D-galactose and 3,6-anhydro-αL-galactose units linked together by glycosidic bonds. It is soluble in an aqueous solution when heated to temperatures >85 °C and forms fibrous aggregates of agarose helices when cooled to the gelation temperature, forming a loose network of agarose fibers.[11] The interactions between the agarose fibers are non-covalent, but have a very high energy barrier, so that once a gel has formed, its structure remains largely unchanged without external influences. However, gel formation is reversible and liquefaction requires temperatures far above the gelation temperature.[12] The mechanical properties and pore size of the gel can be adjusted via the concentration of agarose used and the gelation temperature, whereby higher concentrations and lower gelation temperatures lead to firmer agarose fiber networks with higher stiffness and smaller pores.[12a,13]

To evaluate our indentation platform, we prepared agarose gels by heating aqueous solutions of varying agarose content (0.5–2 % w/v) to 90 °C and then rapidly cooling to a gelation temperature of either 37, 25, or 4 °C. These gels were prepared directly in the 25 mm diameter sample vessels and then analyzed using a 1 mm diameter plunger. A representative force-distance curve of a 1.5 % agarose gel prepared at a gelation temperature of 25 °C is shown in **Figure** 2A. The entire indentation process was carried out at a constant plunger speed of 0.2 mm s^{-1} and the distance (lower x-axis) and depth of indentation (upper x-axis) are shown respectively. Point I indicates the contact when the plunger touches the surface of the agarose gel, followed by a quasi-linear phase II in which the force exerted by the plunger indents the gel. After a certain penetration depth, the force drops abruptly as the gel matrix breaks (III). At this breaking point, the material is physically separated by the force of the plunger, which leads to a relaxation of the material and the observed decrease in the force exerted on the plunger. For a photographic representation of the phases, see Figures S4A,B (Supporting Information).

In addition to tensile and flexure tests, compression tests are the basic mechanical test methods that determine, among other things, the modulus of elasticity, also known as Young's modulus (E), which is a classic material parameter that characterizes the stiffness of materials. Specifically, it describes the proportional

relationship between stress and strain in a solid body that deforms, in the case of linear-elastic behavior. The platform developed here uses a relatively small plunger for the indentation, which is a significant advantage for small-volume samples. However, conventional models used to characterize the material´s response to indentation cannot be applied since assumptions are not met. In order to correlate the measurements of our indentation platform with classical compression tests, we performed tests with gels of different agarose concentrations (0.5–2 % w/v) gelled at 25 °C. Initially, the Young's moduli of these gels were determined by calculating the slope of the linear elastic region of standardized measurements of stress–strain diagrams obtained with a commercially available compression tester (Texture Analyzer TA.XTplus, Stable Micro System, Figure S4C, Supporting Information).[14] Then, the slope of the force–distance curves measured with our custom-made indenter, which gives the stiffness of the material (k), was taken from the linear region at a penetration depth <20 % (phase II in Figure 2A). Since the stiffness is proportional to the Young´s modulus, we determined the relationship between the k values obtained with our platform and the E values obtained with the commercial indenter. The correlation between k and E resulted in a linear equation with the following constants: $k\,[N\,m^{-1}] = 0.27 \cdot E\,[kPa] + 2.40$. The measured values of both test methods within the considered force range showed a very good coefficient of determination ($R^2 = 0.99989$, Figure 2B) and clearly demonstrated that our measurement system provides valid values for measurements of the Young's modulus within this stiffness range. Subsequently, the different agarose gels (0.5–2 % w/v) prepared at different gelling temperatures of 4 and 25 °C were compared (Figure 2C). As expected, the hydrogels showed an increase in stiffness with increasing agarose concentration regardless of the gelation temperature, and a higher stiffness was achieved with the same agarose concentration at the lower gelation temperature. Statistical analyses were carried out to validate the experimental results. The significance differences shown in Tables S3 and S4 (Supporting Information) confirmed the results described. As discussed above, these results are consistent with the literature.[12a,13]

To demonstrate the automation of the measurements possible with our indentation platform and the temporal resolution of the system, the gelation of a hydrogel with 0.5 % agarose at a starting temperature of 37 °C and slow cooling to 27 °C within 15 min was investigated in a time-resolved manner (Figure 2D). During the first 13 min of the gelation process, indentations were taken at intervals of 1.5 min (except the first measurement after 0.8 min) and a final measurement after 60 min. In addition, all measurements were performed at different positions with a distance of 5.3 mm on the same sample (Figure S5, Supporting Information), as the indentation of solid hydrogels leads to localized destruction of the gel matrix. This spatially resolved sample examination was made possible by the automated movement of the robotic arm through the positioning system.

Since it applies primarily to solid materials, the modulus of elasticity during gelation is not suitable for evaluating the entire process. Therefore, we used the fracture point (point III, in Figure 2A; Figure S6, Supporting Information) to get a more detailed insight into the transition from liquid to gel. The measurements showed that after 6.8 min there was a clear increase in the fracture point compared to the previous measurements, indicating the start of gelation. Subsequently, a continuous increase in the fracture point was observed up to ≈14 min, after which no further increase occurred, indicating the end of gelation. Statistical analyses of the values determined for fracture points and the moduli of elasticity were carried out to validate the results. The differences in significance shown in Tables S5 and S6 (Supporting Information) confirmed the results described. The data reflect very well the previously described three-stage gelation process, in which an initial induction phase with nucleation takes place, which in our study was completed after 6.8 min, followed by a gelation phase (here 6.8–12.9 min) and then a pseudo-equilibrium phase (here from ≈14 min), in which the fracture point changes minimally or not at all.[12a] Analysis of gelation using the fracture point is not possible with the conventional rheometer, as the samples are too liquid at the beginning of gelation for adequate measurement. However, to confirm our method of gelation analysis, the agarose gelation under the same conditions was also analyzed with the widely used rotational rheometry by means of time-dependent measurement of the storage and loss moduli (see Figure S7, Supporting Information). Gelation was observed from ≈4 min, which agrees well with the fracture point analysis of our penetration platform, indicating a clear increase at ≈5–6 min (Figure 2D; Figure S6, Supporting Information). Of note, the transition from the second to the third phase is also indicated by the Young's moduli measured between 11 and 14 min (grey bars in Figure 2D; see also Figure S6, Supporting Information). Thus, the data obtained from agarose gels clearly show that our platform is not only suitable for fast quality control and relative comparability analysis in process-intensive applications but also for the absolute determination of viscoelastic material properties.

2.3. Viscosity Measurements of Newtonian Fluids – Viscous Glycerol-Water Mixtures

To demonstrate the versatility of the indentation platform, we investigated its use as a viscometer for measuring viscous and viscoelastic materials and liquids. Viscosity measurements are a reliable method for investigating complex gelation and polymerization processes and are used for quality control in the production of such materials. In order to minimize material costs and labor-intensive sample preparation processes, an economical and sensitive instrument that allows the sampling of small quantities and the performance of high-throughput measurements could bring significant benefits. To adapt the indentation platform for viscosity measurements, the setup described above was used with a narrow sample vessel (diameter 4.5 mm) and a relatively wide plunger (diameter 4.3 mm). The displacement of the liquid through the 100 µm thin gap between the sample vessel and the plunger induces a force specific to the liquid on the plunger, which can be measured by the responding load cell. Test measurements with other assembly geometries (e.g., 4.3 mm plunger and 25 mm sample vessel) resulted in significantly lower measurable forces due to the absence of frictional and capillary forces, so that the thin gap was essential for measuring viscosities.

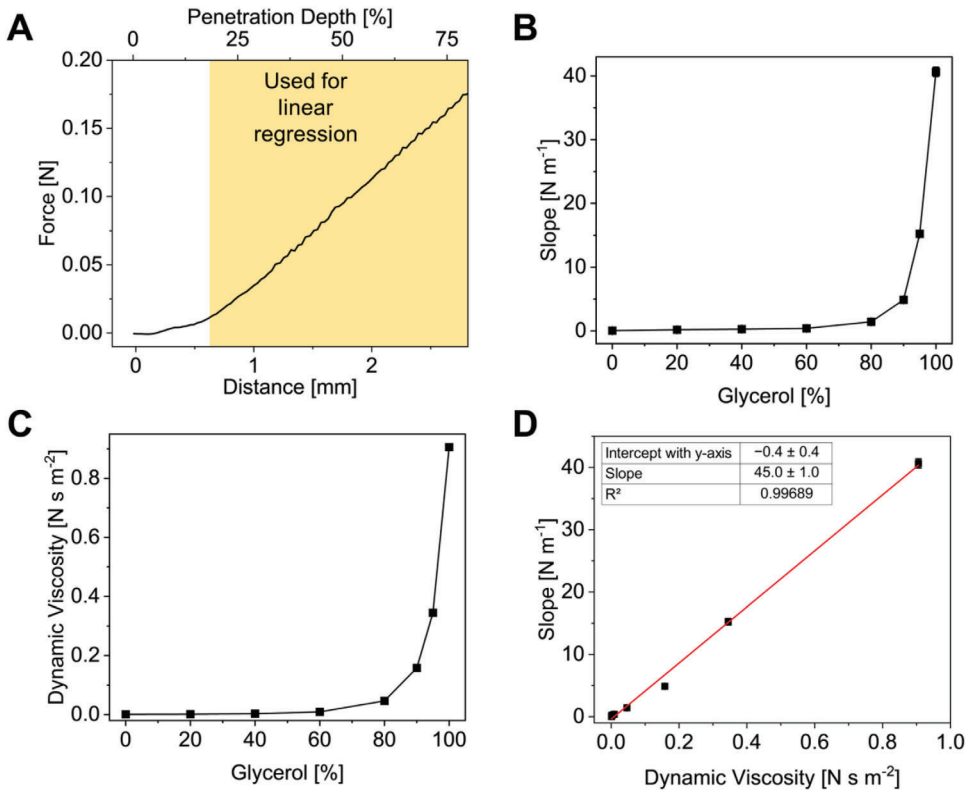

Figure 3. Viscosity measurement of Newtonian fluids. Typically, 75 µL of sample in a 4.5 mm wide sample vessel were measured using a plunger with a diameter of 4.3 mm. A) Representative force–distance curve obtained for 100 % glycerol. The yellow highlighted section shows the linear range that was used for determination of the slope, to enable calibration of the platform to measure dynamic viscosity. B) Results of measuring glycerin-water mixtures using the indentation platform. The diagram shows the slope of the linear measuring range as a function of the glycerol concentration. The measurements were performed in experimental triplicates ($n = 3$) and plotted as the mean ± standard deviation. C) Calculated dynamic viscosity of glycerol–water mixtures as a function of the glycerol concentration according to the mathematical method of Volk and Kähler.[16] D) Calibration curve for the measurement of dynamic viscosity with the novel indentation measurement platform, obtained by correlating the results of (B) and (C). The good fit of the model is underlined by the coefficient of determination R^2>0.99.

Glycerol-water mixtures were chosen as model substances for the viscosity measurements because they are cheap, readily available, and have a Newtonian behavior, which means that the viscosity of the liquid is not affected by an applied force.[15] Therefore, the measured load cell signal is not affected by the speed at which the plunger is immersed in the sample. Since glycerol-water mixtures are well studied and mathematical models for calculating the dynamic viscosity are already described,[16] it should be possible to correlate the measured signal directly with the known viscosity. The measurements of the glycerol-water mixtures (**Figure 3**) were performed at a temperature of 25 °C and an indentation speed of 1 mm s^{-1}. A representative force-displacement curve of the viscous liquid measurement of 100 % glycerol (Figure 3A) shows a steady increase in force throughout the measurement process, with a sharp increase in the measurement signal as soon as the plunger displaces the liquid from the sample vessel. As the plunger penetrates and increasingly displaces the liquid, the viscous frictional force acts in the opposite direction to the movement of the plunger and increases linearly. The yellow highlighted slope area could be used for linear regression analysis. Note that both the distance and penetration depth are shown in the lower and upper x-axes, respectively.

Figure 3B shows the mean forces determined experimentally in triplicates for different glycerol–water mixtures as a function of the glycerol concentration (for representative measurement curves, see Figure S8, Supporting Information). While only a minimal increase in the required force is observed for samples between 0 and 80 % glycerol (slope: 0.05–1.50 N m^{-1}), the forces acting on the load cell increase considerably at glycerol concentrations above 80 % leading to an average slope of ≈40.65 N m^{-1} at 100 % glycerol. The above analysis values correlated well with the model developed by Volk and Kähler to calculate the dynamic viscosity,[16] which showed a very similar trend (Figure 3C). In fact, the quantitative comparison of our experimental results with the theoretically calculated dynamic viscosities provided a linear relationship between the measured slope and the dynamic viscosity (Figure 3D) with a very good coefficient of determination R^2 = 0.99689 and the linear correlation: Slope [N m^{-1}] = 45.0 – Dynamic viscosity [Ns m^{-2}] – 0.4. These results indicated that our platform can be used for meaningful viscosity measurements to compare samples with unknown viscosity relative to each other and that data for absolute dynamic viscosities can also be obtained by calibration as long as the absolute measured values are within the considered range.

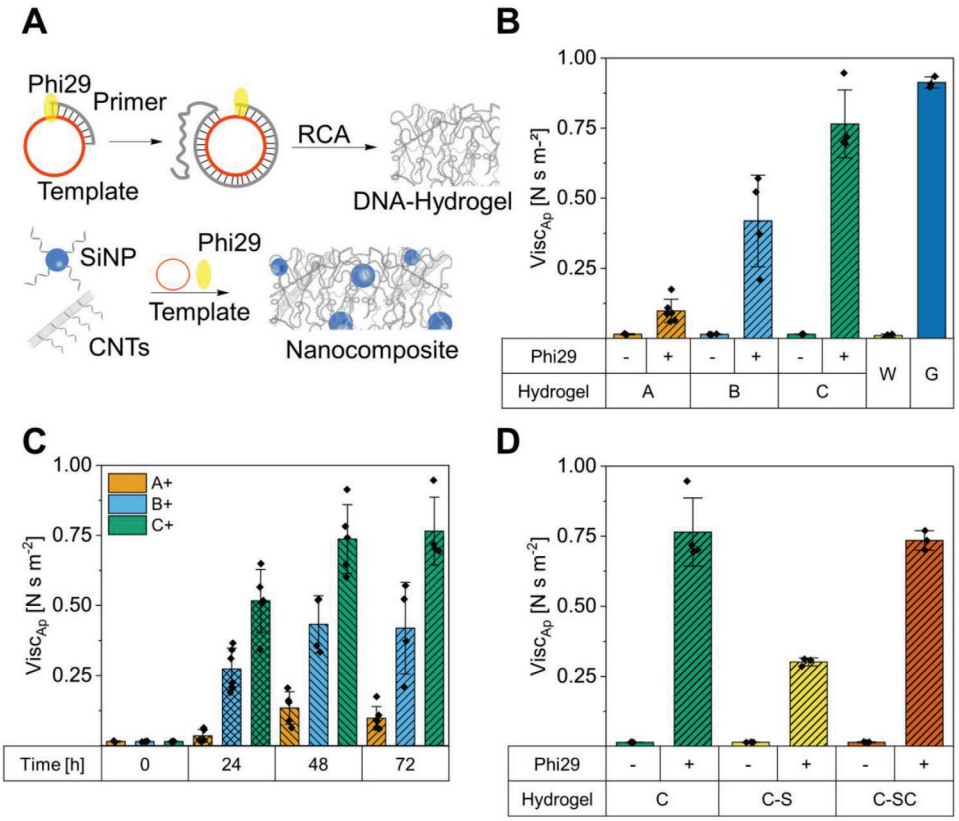

Figure 4. Characterization of RCA-based DNA hydrogels and Nanocomposite materials. A) Schematics of RCA process, wherein Phi29 polymerase elongates a primer hybridized on a circularized template to produce long DNA single strands. For hydrogels purely consisting of DNA (top) a free primer, for nanocomposite materials (bottom) primer-functionalized nanoparticles (SiNP and CNTs) were used. B) Apparent viscosity ($Visc_{Ap}$) values obtained from DNA hydrogels in comparison to water (W) and glycerol (G). Samples indicated with "+" contain polymerase, whereas samples marked "–" are negative controls lacking polymerase. Note that all polymerized samples show a substantially higher $Visc_{Ap}$ than the unpolymerized controls. C) Kinetics of the RCA polymerization process using templates A, B or C, followed in situ over 72 h. Note that $Visc_{Ap}$ increases over time, reaching a plateau after about 48 h. D) Comparison of $Visc_{Ap}$ values of DNA hydrogel C and corresponding nanocomposites C-S and C-SC made from primer-modified SiNP and CNT, respectively). Samples containing or lacking polymerase are marked with "+" or "–", respectively. Note that the RCA-mediated incorporation of carbon nanotubes (C-SC) leads to a higher viscosity than the incorporation of silica nanoparticles (C-S). The measurements (B-D) were conducted in experimental triplicates ($n = 3$) and plotted as the mean ± standard deviation. The dots in Figure B-D represent the individual measurements. For statistical analyses with the corresponding *p*-values, see Tables S7–S13 (Supporting Information).

2.4. Measurements of Non-Newtonian Fluids – Viscoelastic DNA Hydrogels

The approach described above for measuring dynamic viscosity with the indentation platform was then used to study the viscosity of complex biomaterials. Given their great importance for applications in biotechnology, ranging from drug delivery to bioscaffolds for tissue engineering,[3a-f,17] we wanted to investigate DNA-based hydrogels that can be synthesized enzymatically by rolling circle amplification (RCA).[18] As sketched in **Figure 4A**, in the RCA process, Phi29 polymerase extends a primer bound to a circular template to form long DNA single strands with a maximum length of up to 20 000 nucleotides,[19] which intertwine during polymerization to yield very soft, liquid-like viscoeleastic biomaterials with a high water content of typically ≥90 % (see Figure S9, Supporting Information).

Specifically, we selected three different template sequences A, B, and C with different lengths, different GC content, and different proportions of secondary structures at 30 °C. Sequences A and B were previously developed by the Walther group for the preparation of mechanosensitive RCA hydrogels,[20] while sequence C was developed by the Tan group for drug delivery[21] and used by us for the preparation of DNA nanocomposite materials.[4,22] For detailed information on the sequences, see Figure S10 (Supporting Information). Although the materials prepared with templates A, B, and C were difficult to characterize using conventional measurement methods, as they showed high adhesion to small probes and the synthesis of large quantities is very expensive, we first characterized their macroscopic viscoelastic properties, namely storage (G') and loss (G'') moduli, using rotational rheometry (Figure S11, Supporting Information). Hydrogel B and C showed a significant degree of elasticity with G' being always greater than G'' in the whole frequency range investigated (Figure S11B, Supporting Information), indicating the presence of a polymerized network. For hydrogel A, the values of G'' were higher than those of G' over a wide frequency range. It was only at very low frequencies that G' became slightly greater, suggesting a low degree of entanglement of the

network formed. The storage moduli of the DNA hydrogels are considerably lower than those of the agarose gels (see Figures S11 and S12, Supporting Information). Initial experiments with our indentation platform using the same experimental setup as for the agarose measurements did not provide any meaningful signals, indicating that the measurement of the longitudinal elastic modulus of these very soft DNA hydrogels was not possible.

While Newtonian fluids show a constant viscosity independent of the measuring speed, viscoelastic non-Newtonian fluids should show a dependence of the viscosity on the penetration speed of the plunger. Therefore, we first investigated the influence of different indentation velocities (0.2–8 mm s^{-1}) by recording force-displacement curves and plotting their linear slope against the indentation velocity (Figure S13, Supporting Information). The observed nonlinear relationship confirmed that the DNA hydrogels indeed exhibited the viscoelastic properties of a non-Newtonian fluid. Since there are no defined viscosity standards for non-Newtonian fluids that could be used for calibration, we performed all subsequent indentation studies at the same indentation speed already used for the glycerol-water experiments (1 mm s^{-1}) and used the calibration curves obtained with glycerol–water mixtures. In this way, it is possible to determine the apparent viscosity ($Visc_{Ap}$) for the viscoelastic DNA hydrogels, a standard parameter used in industry and research to characterize non-Newtonian fluids.[23] While the apparent viscosity in a Newtonian fluid is constant and corresponds to the dynamic viscosity, the apparent viscosity in non-Newtonian fluids depends on the shear rate, which in this case depends on the penetration rate of the plunger. The apparent viscosity is therefore dependent on the measurement procedure, but allows for comparison of different non-Newtonian fluids if the measurements of the materials were performed under the same conditions.[23]

First, we performed viscosity measurements on hydrogels obtained from templates A, B, and C after 72 h of RCA polymerization according to our previously described protocol[4] (Figure 4B, representative force curves of each hydrogel are shown in Figure S14, Supporting Information). The $Visc_{Ap}$ values of the DNA hydrogels showed viscosity values similar to those obtained for glycerol, while the negative controls, which did not contain Phi29 polymerase, showed $Visc_{Ap}$ values equivalent to those of pure water. These results demonstrate that the successful polymerization can be verified using the indentation measurements. However, the data in Figure 4B and the corresponding statistical analysis (Tables S7 and S8, Supporting Information) showed that the three different DNA hydrogels exhibited strong differences in viscosity, with materials C and B being significantly more viscous than material A.

To confirm these results and to demonstrate the capability of our platform for temporally resolved in situ studies, we performed time-dependent viscosity measurements during RCA synthesis of hydrogels from templates A, B and C (Figure 4C). The study was performed over 72 h by taking an indentation measurement every 24 h. All three materials exhibited an increase in $Visc_{Ap}$ within the first 24 h, which reached a plateau after ≈48 h. Again, the same trend was observed that material C was clearly more viscous than materials B and A. As confirmed by statistical analysis (Tables S9–S11, Supporting Information), the viscosities measured by indentation nicely matched the trend observed with conventional rotational rheometry (Figure S11, Supporting Information).

One possible explanation for the observed differences between DNA hydrogels A–C lies in the amount of DNA polymer chains produced by RCA, which in turn strongly depends on the template sequence. Thus, in a recent work, we found that the absolute amount of RCA product influences the mechanical properties of the hydrogels.[24] In this study, using the same sequences A–C, the concentration of RCA product quantified by qPCR correlated very well with the stiffness of the respective materials. Interestingly, other relative stiffnesses of the hydrogels were observed (A>B>C), which could possibly be due to the parameters (primer, template, and nucleotide concentrations) for the RCA protocol taken from the literature.[20] To investigate this question, we used our new platform here to characterize corresponding DNA hydrogels from sequences A–C prepared according to the above protocol.[20,24] Indeed, we found that the relative stiffness of the hydrogels decreases from A to C (Figure S15, Supporting Information). Thus, this study not only proves the validity of the new indentation method, but also suggests that it can be conveniently used to study these complex biomaterials whose mechanical properties are significantly influenced by various parameters that affect the enzymatic polymerization reaction, such as the concentration of primers, nucleotides, enzymes, the reaction temperature and length, and especially the DNA sequence of the template.[24]

To elaborate on the above aspect and evaluate the relationship between the amount of DNA and the stiffness of the hydrogels synthesized according to the protocol of Hu et al.[4] we quantified the RCA product amount also from these hydrogels by qPCR (Figure S16, Supporting Information). We found that even with this protocol, hydrogel A had the highest DNA content, while hydrogel C had the lowest. Since hydrogel C has the highest apparent viscosity, there is no direct correlation between DNA polymer concentration and mechanical properties. Based on the template sequences of A–C (Figure S10, Supporting Information), it appears that the proportion of secondary structures formed in the amplified DNA plays a significant role. Structural analyses with the webserver Mfold showed that almost 70 % of the bases in hydrogel C are involved in secondary structures, whereas this is only 33 % and 56 % for A and B, respectively.[25] Since these structural elements influence both the synthesis efficacy and the mechanical properties of the final product, more comprehensive modeling will be needed to enable rational structure-property relationships. The indentation method presented here could make an important contribution to the future development of DNA-based materials with customized material properties using machine learning. Progress in this area requires large, high-quality data sets to train neural networks and use them for predictions. Due to its high throughput and spatiotemporal resolution, the indentation method offers the possibility to contribute to the acquisition of the necessary data sets to predict DNA sequences and process parameters that lead to defined mechanical properties of the materials.

As indicated in Figure 4A, RCA-based hydrogels can also be combined with oligonucleotide-functionalized nanoparticles to create nanocomposite materials that have altered material properties.[4,22] To investigate the applicability of the new indentation platform for such complex materials, we prepared

DNA-modified silica nanoparticles (SiNPs) and carbon nanotubes (CNTs) using DNA primers, which were then used as starting points for RCA polymerization. According to previous work, two different materials containing either only SiNP (C-S) or SiNP and CNTs (C-SC) as primers during RCA amplification of circularized template C were prepared using spherical SiNP with a diameter of about 104 ± 14 nm or CNT with a diameter of 2.3 ± 0.5 nm and typical lengths of 216 ± 89 nm.[4] After 72 h of RCA, the $Visc_{Ap}$ values of the obtained materials were determined by indentation measurement (Figure 4D). Force-distance curves showed an immediate clear difference in the slopes, which is then reflected in the calculated viscosity of the materials (for representative examples, see Figure S17, Supporting Information). Compared to the pure DNA hydrogel C, the RCA-based incorporation of primer-modified nanoparticles led to significant changes in the apparent viscosity of the resulting composite materials. It was found that the incorporation of SiNP (material C-S, yellow bars) significantly reduced the viscosity compared to the pure DNA material (hydrogel C, green bars). This result suggests a lower polymerization efficiency due to the particle-bound primers. When CNT was additionally woven into the composite, the direct comparison of the composite materials showed that the CNT-modified material (blue bars) had a significantly higher viscosity than the SiNP-containing material (Figure 4D, for statistical analyses see Tables S12 and S13, Supporting Information). This could be due to the long, stiff CNT particles which, in contrast to the smaller, spherical SiNP, crosslink microscale DNA hydrogel domains more efficiently. Thus, these results again demonstrate the broad applicability of the new indentation method for the characterization of complex biomaterials.

3. Conclusion

In summary, we have developed a new versatile platform for measuring the compressive stress and viscosity of biomaterials. The indentation platform described here enables the measurement of the fracture point and Young's modulus of relatively stiff polymers and the viscosity of particularly soft hydrogels. The setup is highly customizable to sample-specific requirements and measurements can be performed fully automatically, ensuring excellent temporal and spatial resolution. Following the successful characterization of agarose hydrogels with regard to their agarose concentration and gelling temperature, soft DNA hydrogels based on RCA synthesis were also successfully characterized. The apparent viscosity was determined using a water-glycerol calibration. The sensitivity of our method allowed the differentiation of DNA hydrogels prepared with different template sequences, polymerization states during the RCA process, and different synthesis parameters. As shown by DNA hydrogels with interwoven silica nanoparticles and carbon nanotubes, the characterization of more complex nanocomposite materials is also possible. Preliminary experiments with protein-based self-assembling hydrogels indicate that such materials can also be investigated with the indentation platform, for example, to characterize the drying-induced curing of the materials (Figure S18, Supporting Information). We believe that the methodology presented here is a very powerful tool as it combines a high throughput capacity and automation capability with a high degree of flexibility and spatial and temporal resolution. In the future, this will facilitate the characterization of a broad spectrum of complex bioinspired materials systems, improve the reproducibility of synthesis methods, and provide valuable data sets for machine-based modeling and rational prediction of structure-property relationships, thus making valuable contributions to application areas in the life and materials sciences.

Supporting Information

Supporting Information is available from the Wiley Online Library or from the author.

Acknowledgements

P.L. and S.M. contributed equally to this work. This work was financially supported through the Helmholtz Association program "Materials Systems Engineering" under the topic "Adaptive and Bioinstructive Materials Systems" and by the German government, through the BMBF project MicroMatrix (project ID: 161L0284A). S.M. is grateful for a Kekulé fellowship by Fonds der Chemischen Industrie (FCI). The authors thank Julian Hertel and Christoph Bickmann for experimental help with the enzyme foams and the SiNP synthesis and CNT functionalization, respectively, and Prof. Manfred Wilhelm (KIT) for fruitful discussions.

Open access funding enabled and organized by Projekt DEAL.

Conflict of Interest

The authors declare no conflict of interest.

Data Availability Statement

The data that support the findings of this study are available from the corresponding author upon reasonable request.

Keywords

agarose, DNA hydrogels, indentation, mechanical characterization, viscosity, Young's modulus

Received: February 19, 2024
Revised: April 4, 2024
Published online:

[1] a) D. Seliktar, *Science* **2012**, *336*, 1124; b) M. P. Lutolf, J. A. Hubbell, *Nat. Biotechnol.* **2005**, *23*, 47.
[2] P. M. Kharkar, K. L. Kiick, A. M. Kloxin, *Chem. Soc. Rev.* **2013**, *42*, 7335.
[3] a) D. Yang, M. R. Hartman, T. L. Derrien, S. Hamada, D. An, K. G. Yancey, R. Cheng, M. Ma, D. Luo, *Acc. Chem. Res.* **2014**, *47*, 1902; b) J. Li, L. Mo, C.-H. Lu, T. Fu, H.-H. Yang, W. Tan, *Chem. Soc. Rev.* **2016**, *45*, 1410; c) D. Wang, Y. Hu, P. Liu, D. Luo, *Acc. Chem. Res.* **2017**, *50*, 733; d) Y. Hu, C. M. Niemeyer, *Adv. Mater.* **2019**, *31*, 1806294; e) M. Vázquez-González, I. Willner, *Angew. Chem., Int. Ed.* **2020**, *59*, 15342; f) V. Morya, S. Walia, B. B. Mandal, C. Ghoroi, D. Bhatia, *ACS Biomater. Sci. Eng.* **2020**, *6*, 6021; g) R. Zhong, S. Talebian, B. B. Mendes, G. Wallace, R. Langer, J. Conde, J. Shi, *Nat. Mater.* **2023**, *22*, 818; h) R. Hama, A. Ulziibayar, J. W. Reinhardt, T. Watanabe, J. Kelly, T. Shinoka, *Biomolecules* **2023**, *13*, 280.

[4] Y. Hu, C. M. Domínguez, J. Bauer, S. Weigel, A. Schipperges, C. Oelschlaeger, N. Willenbacher, S. Keppler, M. Bastmeyer, S. Heißler, C. Wöll, T. Scharnweber, K. S. Rabe, C. M. Niemeyer, *Nat. Commun.* **2019**, *10*, 5522.
[5] A. Kowalczyk, C. Oelschlaeger, N. Willenbacher, *Polymer* **2015**, *58*, 170.
[6] a) M. R. VanLandingham, *J. Res. Natl. Inst. Stand. Technol.* **2003**, *108*, 249; b) Q. Zhang, in *The Mechanics of Hydrogels* (Eds: H. Li, V. Silberschmidt), Woodhead Publishing, Cambridge, UK **2022**, p. 91.
[7] Y. M. Efremov, T. Okajima, A. Raman, *Soft Matter* **2020**, *16*, 64.
[8] a) M. Papi, G. Arcovito, M. De Spirito, M. Vassalli, B. Tiribilli, *Appl. Phys. Lett.* **2006**, *88*, 194102; b) N. Ahmed, D. F. Nino, V. T. Moy, *Rev. Sci. Instrum.* **2001**, *72*, 2731.
[9] a) S. H. Hansen, T. Kabbeck, C. P. Radtke, S. Krause, E. Krolitzki, T. Peschke, J. Gasmi, K. S. Rabe, M. Wagner, H. Horn, J. Hubbuch, J. Gescher, C. M. Niemeyer, *Sci. Rep.* **2019**, *9*, 8933; b) P. Lemke, A. E. Zoheir, K. S. Rabe, C. M. Niemeyer, *Biotechnol. Bioeng.* **2021**, *118*, 3860.
[10] T. Fujii, T. Yano, H. Kumagai, O. Miyawaki, *Biosci. Biotechnol. Biochem.* **2000**, *64*, 1618.
[11] a) M. Watase, K. Nishinari, *Rheol. Acta* **1983**, *22*, 580; b) Y. Gu, K.-L. Cheong, H. Du, *Chem. Cent. J.* **2017**, *11*, 104.
[12] a) J.-Y. Xiong, J. Narayanan, X.-Y. Liu, T. K. Chong, S. B. Chen, T.-S. Chung, *J. Phys. Chem. B* **2005**, *109*, 5638; b) M. Beaumont, R. Tran, G. Vera, D. Niedrist, A. Rousset, R. Pierre, V. P. Shastri, A. Forget, *Biomacromolecules* **2021**, *22*, 1027.
[13] V. Normand, D. L. Lootens, E. Amici, K. P. Plucknett, P. Aymard, *Biomacromolecules* **2000**, *1*, 730.
[14] S. L. Garrett, in *Understanding Acoustics: An Experimentalist's View of Sound and Vibration*, (Ed: S. L. Garrett), Springer International Publishing, Cham **2020**, p. 179.
[15] G. K. Batchelor, *An Introduction to Fluid Dynamics*, Cambridge University Press, Cambridge **2000**.
[16] A. Volk, C. J. Kähler, *Exp. Fluids* **2018**, *59*, 75.
[17] J. Gačanin, C. V. Synatschke, T. Weil, *Adv. Funct. Mater.* **2020**, *30*, 1906253.
[18] J. B. Lee, S. Peng, D. Yang, Y. H. Roh, H. Funabashi, N. Park, E. J. Rice, L. Chen, R. Long, M. Wu, D. Luo, *Nat. Nanotechnol.* **2012**, *7*, 816.
[19] L. Blanco, A. Bernad, J. M. Lázaro, G. Martín, C. Garmendia, M. Salas, *J. Biol. Chem.* **1989**, *264*, 8935.
[20] R. Merindol, G. Delechiave, L. Heinen, L. H. Catalani, A. Walther, *Nat. Commun.* **2019**, *10*, 528.
[21] G. Zhu, R. Hu, Z. Zhao, Z. Chen, X. Zhang, W. Tan, *J. Am. Chem. Soc.* **2013**, *135*, 16438.
[22] a) Y. Hu, C. M. Niemeyer, *J. Mater. Chem. B* **2020**, *8*, 2250; b) Y. Hu, D. Rehnlund, E. Klein, J. Gescher, C. M. Niemeyer, *ACS Appl. Mater. Interfaces* **2020**, *12*, 14806.
[23] a) F. J. Galindo-Rosales, F. J. Rubio-Hernández, A. Sevilla, *J. Non-Newton. Fluid Mech.* **2011**, *166*, 321; b) S. Thammakiti, M. Suphantharika, T. Phaesuwan, C. Verduyn, *Int. J. Food Sci. Technol.* **2004**, *39*, 21; c) T. C. Davenport, *Phys. Educ.* **1968**, *3*, 139.
[24] L. Schneider, M. Richter, C. Oelschlaeger, K. S. Rabe, C. M. Domínguez, C. M. Niemeyer, *Chem. Commun.* **2023**, *59*, 12184.
[25] M. Zuker, *Nucleic Acids Res.* **2003**, *31*, 3406.

